energies

Article

Distribution Characteristics of Micro Remaining Oil of Class III Reservoirs after Fracture Flooding in Daqing Oilfield

Nan Jiang [1], Zilu Zhang [2,3,*], Guohui Qu [2,3], Jiqiang Zhi [2,3] and Rongzhou Zhang [2,3]

1 School of Electrical Engineering & Information, Northeast Petroleum University, Daqing 163318, China; dqjiangnan@nepu.edu.cn
2 School of Petroleum Engineering, Northeast Petroleum University, Daqing 163318, China; quguohui@nepu.edu.cn (G.Q.); zhijiqiang@nepu.edu.cn (J.Z.); sygczrz@stu.nepu.edu.cn (R.Z.)
3 Key Laboratory of Enhanced Oil Recovery, Northeast Petroleum University, Ministry of Education, Daqing 163318, China
* Correspondence: zhanglaoban@stu.nepu.edu.cn

Abstract: The class III reservoir in the Daqing Oilfield has poor sand body development, poor reservoir physical properties, and poor effects of measures. Its water drive recovery degree is low and the remaining reserves are large. It is the key target oil layer of the Daqing Oilfield. Due to the sedimentary characteristics and reservoir physical properties of class III reservoirs, conventional EOR technology (chemical flooding) and conventional stimulation and injection measures (fracturing) have poor potential tapping effects on class III reservoirs. According to the special reservoir conditions and development characteristics of the class III reservoir in the Daqing Oilfield, fracture-flooding technology is innovatively proposed, which greatly improves the recovery of remaining oil in class III reservoirs. The rapid injection of hydraulic surface activators into the formation and displacement of the remaining oil in class III reservoirs through rock core flooding experiments were simulated in this paper. The nuclear magnetic resonance (NMR), confocal scanning laser, and computed tomography (CT)-scanning technologies were applied to study the remaining oil distribution after fracture flooding. The results show that: (1) After fracture flooding, the peak value of the T_2 spectrum curve of NMR shifts to the left and the degree of middle and small pore space production increases obviously. (2) Confocal scanning laser study shows that the remaining oil in thin membranous and clustered forms on pore surfaces is highly utilized. (3) CT scan study shows that the remaining oil in membranous and clustered forms is effectively utilized after fracture flooding. In summary, fracture-flooding technology can improve the washing efficiency and sweep volume of class III reservoirs, thus enhancing the recovery efficiency of class III reservoirs.

Keywords: fracture flooding; microscopic residual oil; NMR; laser scanning confocal; computed tomography scan

check for updates

Citation: Jiang, N.; Zhang, Z.; Qu, G.; Zhi, J.; Zhang, R. Distribution Characteristics of Micro Remaining Oil of Class III Reservoirs after Fracture Flooding in Daqing Oilfield. *Energies* **2022**, *15*, 3385. https://doi.org/10.3390/en15093385

Academic Editor: Mofazzal Hossain

Received: 18 March 2022
Accepted: 26 April 2022
Published: 6 May 2022

Publisher's Note: MDPI stays neutral with regard to jurisdictional claims in published maps and institutional affiliations.

Copyright: © 2022 by the authors. Licensee MDPI, Basel, Switzerland. This article is an open access article distributed under the terms and conditions of the Creative Commons Attribution (CC BY) license (https://creativecommons.org/licenses/by/4.0/).

1. Introduction

Due to the serious interlayer heterogeneity, poor reservoir physical properties, and low water-flooding recovery degree of class III reservoirs, the remaining oil is mainly distributed in thin and poor reservoirs with small effective thick bottoms, low permeability and outer surface reservoirs, and large remaining oil potential [1]. Due to the serious heterogeneity of class III reservoirs and the development methods of water flooding and chemical flooding, the recovery degree of class III reservoirs is low and the development effect is poor. In order to effectively exploit the remaining oil of a class III reservoir, it is necessary to increase the injection production pressure difference, control the fluidity, and reduce the oil–water interface tension of the class III reservoir. Due to the poor physical properties of the reservoir, the injection efficiency of conventional enhanced oil recovery technology (chemical flooding) is low, the injection parameters do not match, the production effect is poor, the development effect is limited, the viscosity loss rate of the chemical agent is high, the loss of agent performance along the way (adsorption and retention) is large, and the displacement effect is not ideal [2,3]. After fracturing the class III reservoir by conventional fracturing processes, due to the poor production degree of the fractured layer, low water drive connectivity, and low reservoir energy, it is impossible to establish an effective displacement relationship, short fracturing validity period, low cumulative oil increase, and poor stimulation effect. Fracture-flooding technology based on large-scale fracturing was proposed to solve the problems of low-permeability reservoirs' physical properties and fracture formation fracture morphology in the Daqing Oilfield [4]: a surface active agent as fracturing fluid was rapidly advanced to the deep reservoir by hydraulic fracture flooding and enriching and exploiting remaining oil to realize highly efficient oil displacement. However, due to the coupling effect of hydraulic fracturing and fracturing fluid seepage and oil displacement in fracture-flooding technology, there is still a lack of research on the utilization of remaining oil in fracture flooding.

At present, there are two main models for the research and analysis of micro residual oil distribution characteristics: (1) Using core thin sections, the distribution characteristics of micro residual oil are mainly studied using computed tomography (CT) scanning, NMR, and laser confocal technologies. Tan et al. [5] took the actual core samples of the conglomerate reservoir in the Karamay Oilfield as the research object and applied CT-scanning technology to study the micro residual oil distribution law of water flooding and polymer flooding of hydrophilic rock and lipophilic rock. Chen et al. [6] conducted pore-scale multi-phase flow experiments on sandstone core samples and studied the effect of chemical oil displacement on pore-scale wettability controlled by water film propagation through CT-scanning technology. Liu et al. [7] selected cores with different lithologies such as sandstone and glutenite for NMR experiments to study the production and distribution characteristics of micro residual oil in polymer flooding. Liu et al. [8] studied the micro residual oil distribution characteristics of chemical flooding using the visual conglomerate stratification model and NMR experiments to quantify the micro residual oil distribution of chemical flooding. Liang et al. [9] analyzed the types, distribution characteristics, and formation mechanism of micro residual oil in the reservoir after ASP flooding using laser confocal scanning microscope technology and a microphysical simulation experiment. Xia et al. [10] combined the laser confocal and core fluorescence analysis technologies with a core oil displacement experiment to study the distribution characteristics of core oil and water and the microgenesis of remaining oil in view of the lack of research on the distribution characteristics and quantitative characterization of reservoir oil and water. Li et al. [11] revealed the oil displacement mechanism and the remaining oil distribution law of the combined oil displacement system through visual simulation experiments and scanning electron microscopy. Aiming at the research on the micro residual oil distribution characteristics of chemical flooding and enhanced displacement, Zhou et al. [12] quantitatively analyzed the micro residual oil distribution in the pore throat after the water flooding of different rock samples, different displacement stages, and different water injection multiples through a micro displacement experiment of a nuclear magnetic resonance imaging core. A water-flooding experiment carried out by Gao et al. [13] with the improved NMR high-pressure displacement system has defined the occurrence state of remaining oil and qualitatively analyzed and quantitatively evaluated the main factors affecting water flooding efficiency; Bai et al. [14] quantitatively determined the spatial distribution characteristics of micro residual oil after polymer flooding by using new methods of frozen film making, UV fluorescence, and CT nondestructive analysis; Liu et al. [15] used laser confocal technology to determine the micro distribution law of remaining oil after ASP flooding; Xu Q.H. [16] used laser confocal microscope (LSCM) two-dimensional- and three-dimensional-imaging technology to qualitatively and quantitatively determine the micro residual oil distribution characteristics based on coring wells after ASP flooding; Wang et al. [17] determined the distribution characteristics and availability of micro residual oil in polymer flooding by means of a core displacement experiment, frozen production technology, and core fluorescence analysis; Zhang S.Q [18] combined CT-scanning technology with the laboratory experiment of polymer/surfactant composite flooding and understood the pore structure and residual oil change law of polymer/surfactant composite flooding in different stages by CT scanning the cores in different stages. (2) Through the visual model of glass etching, Xia et al. [19] studied the influence of interface characteristics of a ternary composite system on oil displacement efficiency by using the micro visual model. Reducing interface tension and interface viscoelasticity is conducive to emulsifying residual oil and improving oil displacement efficiency. Liu et al. [20] used the simplified pore model to simulate the formation pore structure. According to the occurrence state and distribution characteristics of micro residual oil in the model after displacement by different oil displacement systems, the micro visual oil displacement system was used to calculate the residual oil saturation in the model.

In order to further clarify the occurrence state and distribution characteristics of micro residual oil in fracture flooding, this paper simulates the oil displacement process of fracture flooding through a displacement experiment and quantitatively characterizes the micro residual oil (the remaining oil production in different pore spaces is studied by NMR technology; the quantitative parameters of different types of micro residual oil are determined by confocal-scanning-laser and CT-scanning technologies). Based on the variation of micro residual oil and the morphology of different types, the formation reasons of microscopic remaining oil are studied to provide theoretical support for the effective development of the class III reservoir.

2. Fracture-Flooding Technology

The buried depth of the class III reservoir in the Daqing Oilfield is relatively shallow (<1500 m), and the principal horizontal stress is greater than the principal vertical stress. According to the fracture opening theory [21], the fractures in the Daqing Oilfield are horizontal fractures [22,23]. The results of fracture microseismic monitoring show that the fractures in the Daqing Oilfield are horizontal fractures (Figure 1). Horizontal fractures protect fracturing fluid from infiltrating and filling the formation after fracture flooding.

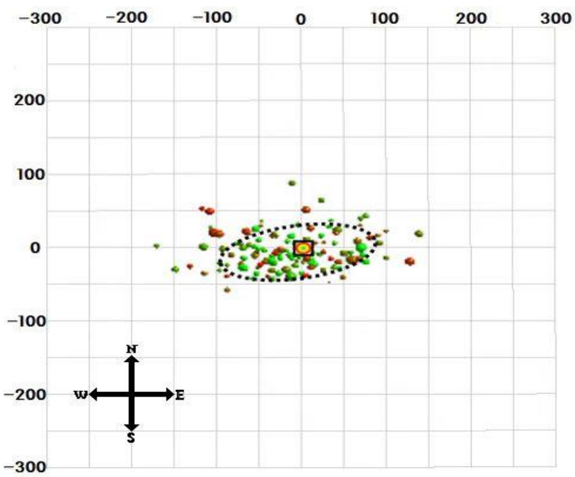

Figure 1. Downhole microseismic interpretation results.

The fracture-flooding technology injected fracturing fluid through fracturing at the production side (oil well) and applied fracture extension to drive the fracturing fluid to the formation pores along the upper and lower side faces of the fracture and the fracture site [24]. After the fracture flooding process, the oil well was stewed to make the fracturing fluid diffuse in the formation and then injected into the well to restore the conventional oil displacement method [25,26]. Fracture-flooding technology can reduce the contact distance and contact time of chemical agents in the formation, solve the performance loss along the way in chemical agent injection, and improve the utilization efficiency of chemical agents. Fracture-flooding also can rapidly increase the formation pressure, establish effective displacement between oil and water wells, and achieve the starting pressure gradient of a low-permeability oilfield. Then, the conventional oil displacement method was adopted to displace the remaining oil to achieve the uniform displacement of high- and low-permeability layers, thus improving oil recovery. The fracture flooding process was designed as the construction procedure flow of fracturing fluid's direct fracture making, step-change displacement (to gradually increase displacement), and slug intermittent injection to pursue fracture extension and maximize the filtration of fracturing fluid. The schematic diagram of the fracture flooding process is shown in Figures 2 and 3.

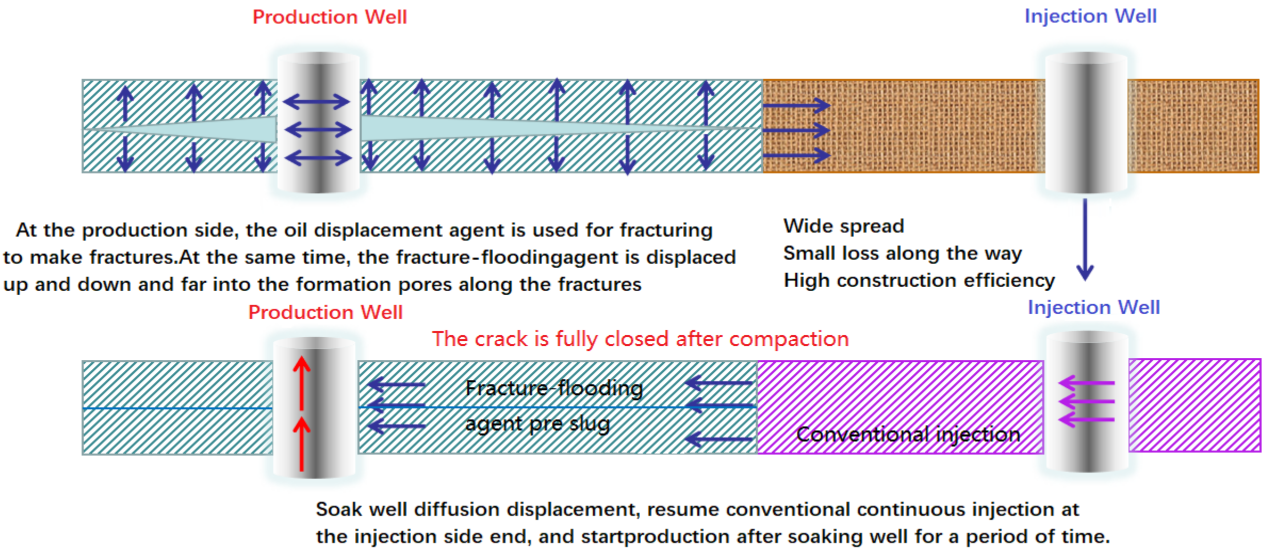

Figure 2. Schematic diagram of fracture flooding.

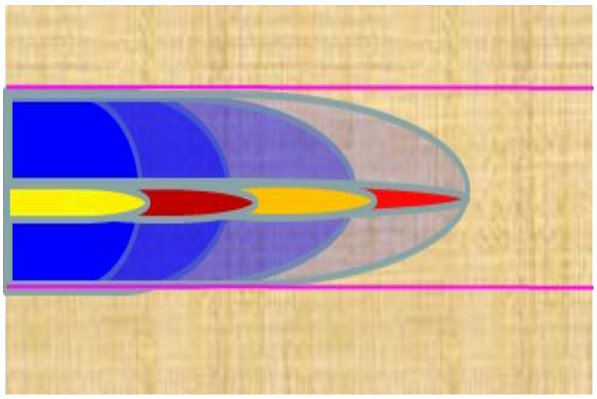

Figure 3. Schematic diagram of fracture propagation and fracturing fluid filtration during fracture flooding.

Due to the serious heterogeneity of the class III reservoir, conventional fracturing can only improve reservoir permeability but cannot establish the effective displacement differential pressure between the oil well low-permeability reservoir and the corresponding water well. Even after the fracturing of the oil well low-permeability reservoir, the energy in the near-well area is insufficient, the remaining oil cannot be effectively developed, and the oil increase effect is poor. Compared with the conventional fracturing process, since the fracturing fluid for fracture flooding is a high-efficiency oil displacement agent (surfactant and surface polymerization agent), fracture-flooding technology and conventional fracturing technology have changed in fracture propagation and the oil displacement mechanism: (1) The "fluid loss reduction" is transformed to the "fluid loss promotion". The conventional fracturing fluid (guar gum) is mainly for forming fractures. Therefore, the fracturing design needs to reduce the filtration loss to reduce the damage to the reservoir. However, the fracturing fluid (surfactant) for fracture flooding is directly pressed into the formation, which needs to increase the spread range of the fracturing fluid in the reservoir. (2) "Promoting extension" is changed to "slow extension". Conventional fracturing mainly focuses on increasing fracture length and expanding fracturing area. While fracture flooding requires fracture extension, fracturing fluid (chemical agent) shall be filtered into the reservoir as much as possible. (3) "Fast flowback" is turned to "slow diffusion". After conventional fracturing, it is necessary to quickly flow back to reduce the damage of fracturing fluid, while fracture flooding requires a chemical agent to diffuse into the oil layer to make the surfactant fully in contact with the formation and reduce the interfacial tension to improve oil recovery.

3. Study on the Distribution Characteristics of the Microscopic Remaining Oil in Fracture-Flooding

3.1. Design of Fracture-Flooding Experiment Scheme

3.1.1. Experimental Materials

The fracturing fluid used in the experiment was petroleum sulfonate with a 0.3% mass concentration (oil–water interfacial tension 3.4 $mN \cdot m^{-1}$). The water used to prepare surfactant was used for fracturing fluid in the field construction of Daqing Oilfield downhole operation company. The experimental oil with a viscosity of 9.75 mPa·s at 45 °C was simulated oil mixed with kerosene after degassing and dehydration of the produced oil from the low-permeability reservoir in Daqing Sazhong development zone. The experimental water was injected into the formation water of the third oil layer in the Daqing Oilfield with a salinity of 3681 $mg \cdot L^{-1}$. The natural cores used in the experiment (diameter: 2.5 cm, no cracks, drying) were all collected from class III reservoir layers in the Daqing Oilfield. The layers experienced the water flooding development stage, but the recovery degree was low. The core samples were provided by the core reference office of Daqing Oilfield exploration and development research institute.

3.1.2. Experimental Equipment

High-temperature and high-pressure reservoir displacement simulation device, MicroMR12 NMR instrument, laser scanning confocal microscope (LSCM, model LEICA SP5II), and Micro XCT-400 CT machine with CT scan image data-processing software Avizo 8.0 were used in this experiment. In addition, double-cylinder constant-speed constant-pressure pump (HBS300/50), piston vessel, pressure sensor (0.01~40 MPa), core gripper, thermostat, hand pump (GJB-II), vacuum pump (2XZ-4), timer, electronic balance (WTB5003), agitators (JB200-SH), caliper, measuring test pipe, etc., were also used.

3.1.3. Experimental Design Scheme

As can be seen from the process of fracture flooding (Figure 2), fracture flooding mainly involves fracturing the production well after water flooding by infiltrating the fracturing fluid (surfactant) into the reservoir pore under the net pressure along the fracture as the fracture expands. The fracture flooding process is characterized by a high-pressure and high-speed core displacement experiment, and the experimental design diagram is shown in Figure 4. The water flooding stage core displacement adopted constant speed displacement. After the core injection and production sides were turned over, high-pressure and high-speed displacement was carried out to simulate fracturing fluid injection into the reservoir after fracture flooding of the production side. According to the similarity criterion [27,28], the experimental parameters related to the displacement core experiment of water flooding and fracture flooding were determined.

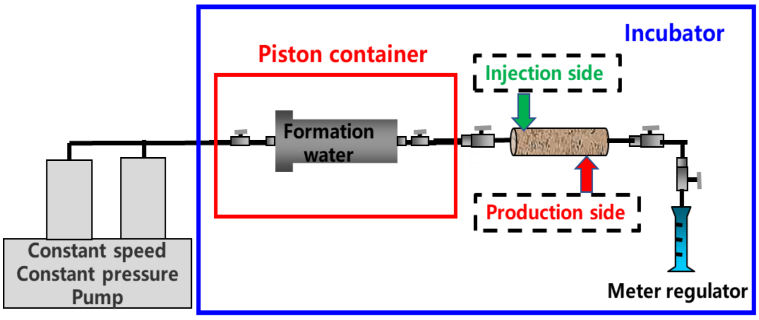

Schematic diagram of water flooding core displacement experimental device.

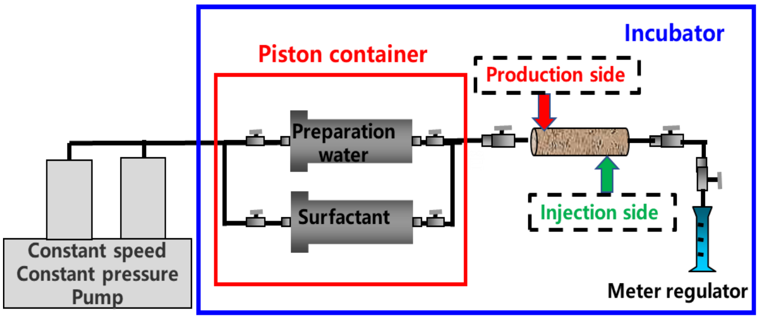

Schematic diagram of core displacement experimental device for fracture flooding.

Figure 4. Design diagram of core displacement experiment scheme for fracture flooding.

3.2. Distribution Characteristics of Microscopic Remaining Oil

3.2.1. NMR Technology

(1) Experimental Method

NMR technology was applied to characterize water saturation changes in different pores through the relaxation characteristics of water in pores. The fluid distribution in the displacement process reflected the distribution of pore size, and the NMR T_2 spectrum was obtained by Fourier transform fitting. NMR T_2 spectrum was converted into a pore radius distribution curve to obtain the relationship between pore radius and T_2 value. Thus, the production of pore crude oil in the reservoir core could be evaluated by NMR data [29,30]. The T_2 relaxation times of different pores were different. T_2 relaxation times less than 10 ms ranged from 10 ms to 100 ms, and times greater than 100 ms were defined as small pores, medium porosity, and macropore, respectively. The surrounding area of the T_2 spectrum curve corresponds to the fluid volume. The change of T_2 can be used to evaluate the fluid production in the pores [31].

(2) Experimental Procedures

The natural core data obtained in the experiment are shown in Table 1. The experiment was carried out after oil washing and drying. The NMR experiment was performed according to SY/T6490-2014 Specification for Laboratory Measurement of NMR Parameters of Rock Samples (oil and gas industry standard). The experimental procedures are as follows:

- Before the experiment, the rock core was cut to about 5 cm and dried at 110 °C to measure core length and diameter and physical parameters such as conventional porosity and permeability. The core was vacuumed, and the saturated formation water was pressurized. Then, the core was measured by NMR in saturated water T_2 spectrum.
- Saturated oil and bound water, displacement speed of 0.1 mL/min, and co-displacement of about 15 pore volume were used (PV). The T_2 spectrum of core was measured by NMR with saturated oil and bound water to record the volume of produced water and calculate the bound water saturation.

- The displacement speed of the water flooding was 0.1 mL/min, and no oil was produced at the producing side. The T_2 spectrum of the core was measured using NMR at this state.
- After fracture flooding, surfactant displacement was performed through high-pressure and high-speed injection from the reverse direction (water flooding production side) with displacement pressure at 2 MPa and injection volume of 0.3 PV. The T_2 spectrum of the core was measured using NMR at this state.

Table 1. Basic data of NMR core.

Well Identifier	Core No.	Permeability ($\times 10^{-3}$ μm^2)	Porosity (%)	Bound Water Saturation (%)
G111-J455	1-1	119.4	24.18	35.43
N5-21-741	2-1	103.5	22.46	35.04
X2-1-729	3-1	88.4	23.85	34.87

(3) Distribution Characteristics of Microscopic Remaining oil NMR Results of Different Core Displacement Stages Are Shown in Figure 5:

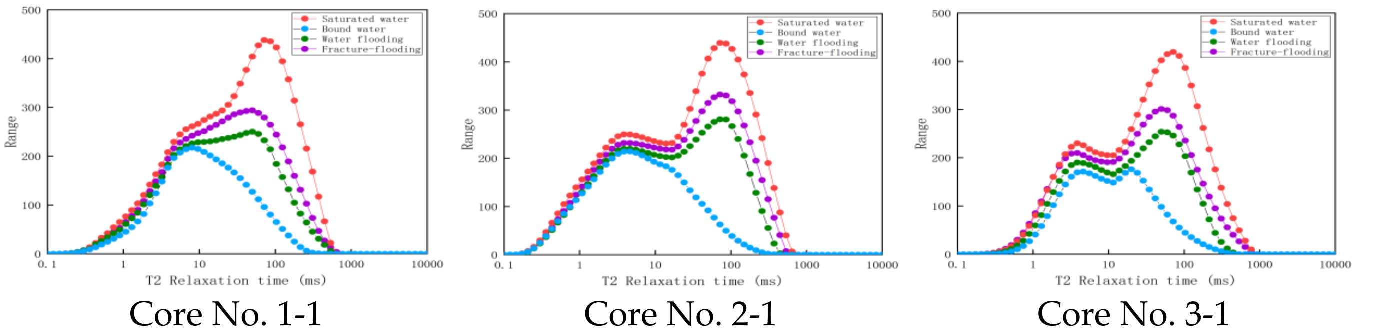

Figure 5. NMR T_2 spectrum curves of different displacement states.

After water flooding, the recovery degree of macropores is 43.38% (Figures 6 and 7, Table 2). The results are mainly because of the small seepage resistance in macropores and the easy flow of fluid in macropores; in addition, the formation of preferential passage at the macropores after water is seen at the exit end results in low development and utilization degree of small and middle pores (33.13% for middle pores and 19.09% for small pores) and large distribution of remaining oil. After fracture flooding, the peak value of the spectrum curve shifts to the left, and the utilization degree of small and middle pores is significantly improved (49.40% for middle pores and 40.91% for small pores). The phenomenon is mainly because the emulsification of fracturing fluid (surfactant), the reduction of interfacial tension, and the high-speed displacement of fracture flooding make the remaining oil in the small and middle pores effectively utilized. With the decrease in oil–water interfacial tension and hydrophilicity, the seepage resistance decreases and the oil phase seepage capacity of small and medium pores increases. Increasing the injection speed can improve the sweep area of crude oil. After enlarging the production pressure difference, some parts of crude oil with low permeability, large start-up pressure, and no flow of crude oil can overcome the seepage resistance and start to flow, increasing the sweep volume of small and middle pores.

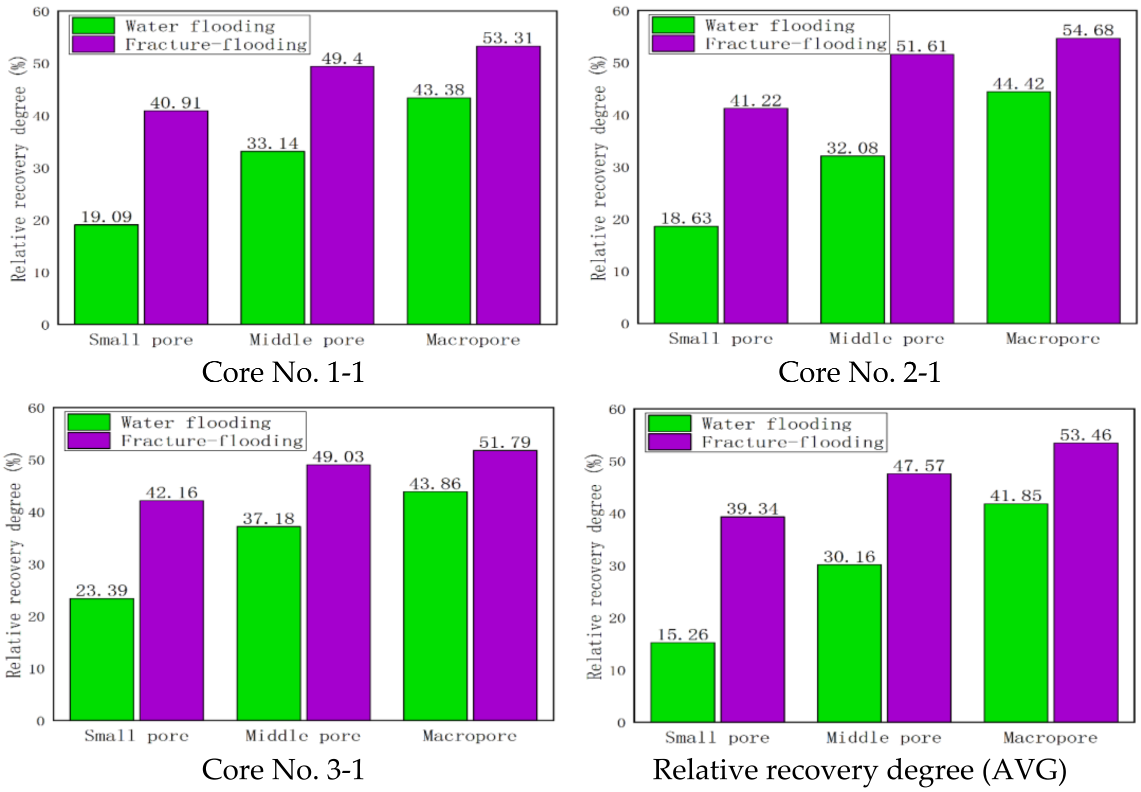

Figure 6. Relative recovery degree under different displacement conditions.

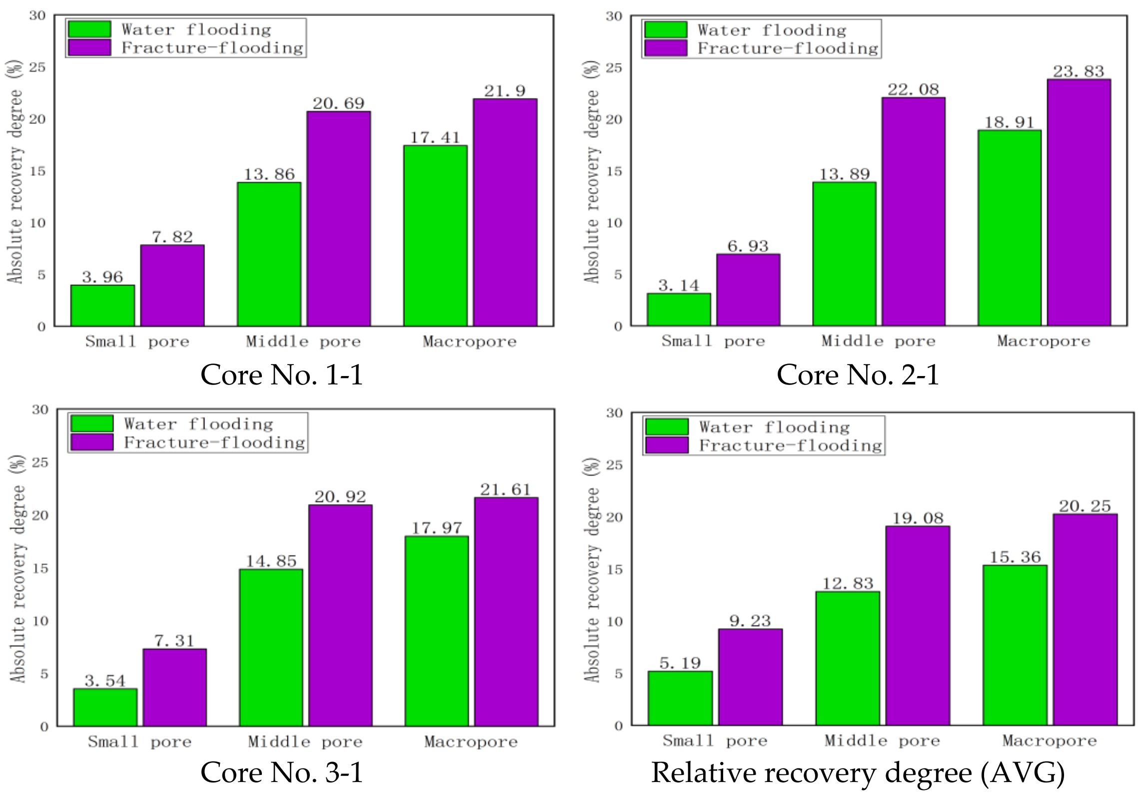

Figure 7. Absolute recovery degree under different displacement conditions.

Table 2. Recovery degree table of different pore areas of T_2 spectrum under different displacement states.

Core No.	Displacement State	Recovery Degree (%)	Absolute Recovery Degree (%)			Relative Recovery Degree (%)		
			Small Pore (<10 ms)	Middle Pore (10–100 ms)	Macropore (>100 ms)	Small Pore (<10 ms)	Middle Pore (10–100 ms)	Macropore (>100 ms)
1-1	Water flooding	35.94	3.14	13.89	18.91	18.63	32.08	44.42
	Fracture-flooding	52.84	6.93	22.08	23.83	41.22	51.61	54.68
2-1	Water flooding	36.36	3.54	14.85	17.97	23.39	37.18	43.86
	Fracture-flooding	49.84	7.31	20.92	21.61	42.16	49.03	51.79
3-1	Water flooding	33.38	5.19	12.83	15.36	15.26	30.16	41.85
	Fracture-flooding	48.56	9.23	19.08	20.25	39.34	47.57	53.46
AVG	Water flooding	35.23	3.96	13.86	17.41	19.09	33.14	43.38
	Fracture-flooding	50.41	7.82	20.69	21.90	40.91	49.40	53.31

3.2.2. Laser Scanning Confocal Technology

(1) Experimental Method

The core samples after displacement were made into thin slices. Before slicing, the samples were frozen in liquid nitrogen and then the thin slices were scanned under the laser scanning confocal microscope [32]. The two-dimensional image of the sample was collected using a specific wavelength laser as the emission light source and then was processed by special computer software to finally obtain the two-dimensional and three-dimensional images of the sample [33].

(2) Experimental Procedures

- Natural cores of class III reservoir in Daqing Oilfield (Table 3) were selected for core saturation at 45 °C.
- Water flooding: The core was flooded to 90% water content. The sample was made into thin slices. The remaining oil saturation, oil/water area, and different types of remaining oil of the sample were analyzed using computer image processing and confocal scanning laser technologies.
- Fracture-flooding: Surfactant (0.3 PV) was injected at the reverse high pressure (2 MPa) at the production side of water flooding. The remaining oil saturation, oil/water area, and remaining oil content of different types of samples were observed by confocal scanning laser technology.

Table 3. Basic data of physical properties of confocal scanning laser natural core.

Well Identifier	Core No.	Permeability ($\times 10^{-3}$ μm^2)	Porosity (%)	Bound Water Saturation (%)
G111-J455	1-2	106.5	24.03	34.77
N5-21-741	2-2	86.7	23.76	36.48
X2-1-729	3-2	121.6	24.65	33.56

(3) Types and Distribution Characteristics of Remaining Oil

The types and distribution characteristics of the remaining oil were analyzed through the confocal scanning laser image. The schematic diagram of the remaining oil types in the confocal scanning laser experiment shows that the remaining oil types are divided into three types:

The first type is the free remaining oil (Figure 8), i.e., the remaining oil far from the surface of the hole wall, including the cluster-like type and intergranular adsorption-like type remaining oil. The remaining oil in clustered is mainly distributed in the pores in the form of beads and clustered. The remaining oil of intergranular adsorption is mainly distributed in the parts with high content of clay minerals or intergranular mud impurities.

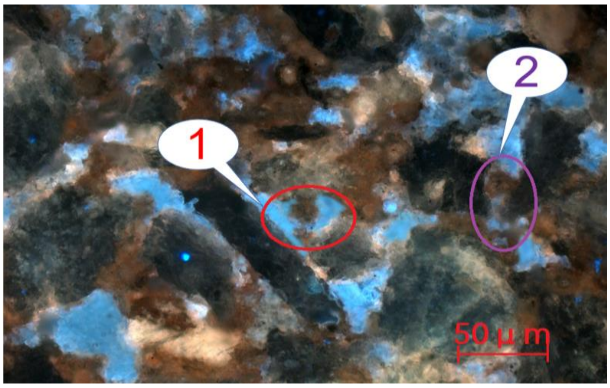

1-Cluster-like type remaining oil; 2-Intergranular adsorption-like type remaining oil.

Figure 8. Schematic diagram of free-state remaining oil types.

The second type is the remaining oil in a bound state (Figure 9), i.e., the remaining oil adsorbed on the surface of the pore wall, including membrane-like and column-like type, slit-like type, and particle-adsorbent-like type remaining oil. The membrane-like and column-like type remaining oil is the membranous remaining oil adsorbed on the surface of rock and mineral particles in the form of membranes. Slit-like type residual oil mainly occurs in a thin and long narrow gap (less than 0.01 mm). Particle adsorbent-like type remaining oil is mainly spread and disseminated on the surface of rock and mineral particles by means of adsorption.

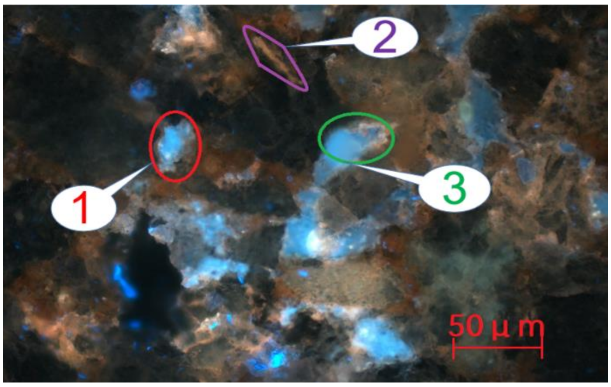

1-Membrane-like and column-like type remaining oil; 2-Slit-like type remaining oil; 3-Particle-adsorbent-like type remaining oil.

Figure 9. Schematic diagram of remaining oil types in a bound state.

The third type is semi-bound remaining oil (Figure 10), i.e., remaining oil outside the bound or relatively far from the surface of the hole wall, including corner-shaped type and throat-like type remaining oil. The corner-shaped type remaining oil is mainly distributed in the corner of the complex pore space. One side is located in the angle depression of the pore, and the other side is in the free state of the external space. The throat-like type remaining oil occurs in the small throat with pore connectivity and often occurs in the slender and curved throat due to capillary action.

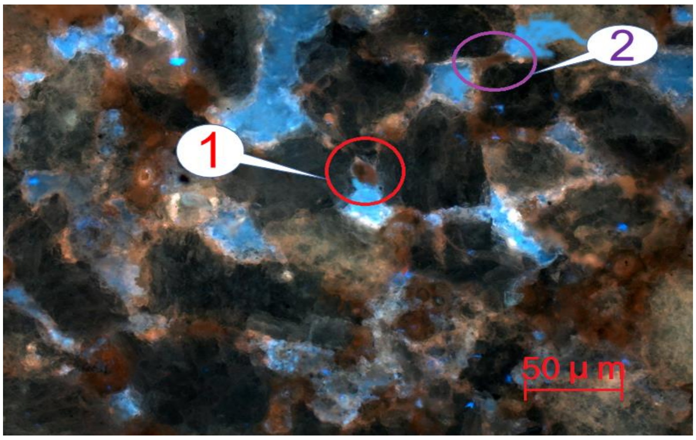

1-Corner-shaped type remaining oil; 2-Throat-like type remaining oil.

Figure 10. Schematic diagram of remaining oil types in a semi-bound state.

(4) Analysis of Microscopic Remaining Oil Distribution in Different Displacement Stages

In order to analyze the oil displacement mechanism of water flooding and fracture flooding and remaining oil distribution characteristics, water flooding and fracture flooding displacement experiments were carried out on natural cores and confocal scanning laser analysis was conducted on cores. The remaining oil distribution is shown in Figure 11. After water flooding, the remaining oil content is large, mainly distributed on the surface of rock particles and intergranular pores. After fracture flooding, the fine remaining oil decreases significantly, the remaining oil on the particle surface is driven out in large quantities, and the cluster-like type remaining oil is reduced to some extent. However, some remaining oil still accumulates in large chunks, indicating that the remaining oil reaccumulates under the action of fracturing fluid. The comparison between the distribution characteristics of the remaining oil in water flooding and that in fracture flooding shows that the remaining oil after fracture flooding is mostly distributed in the form of clusters, while the remaining oil in fine fragments is less. The results indicate that the displacement effect of fracture flooding on remaining oil with small and middle pores is significant.

After water flooding and fracture flooding, sample slices were prepared. Confocal scanning laser technology was used to construct a three-dimensional remaining oil distribution map of rock samples. The content, saturation, and oil/water volume of different types of remaining oil were analyzed by computer image intelligent recognition technology. Table 4 and Figure 12 show the relative percentage of microscopic remaining oil distribution of various types of rock samples.

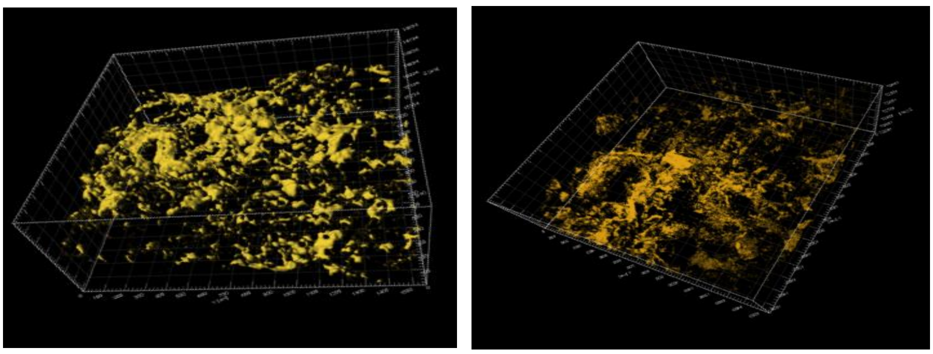

Water flooding stage Fracture-flooding stage

Core No. 1-2

Figure 11. *Cont.*

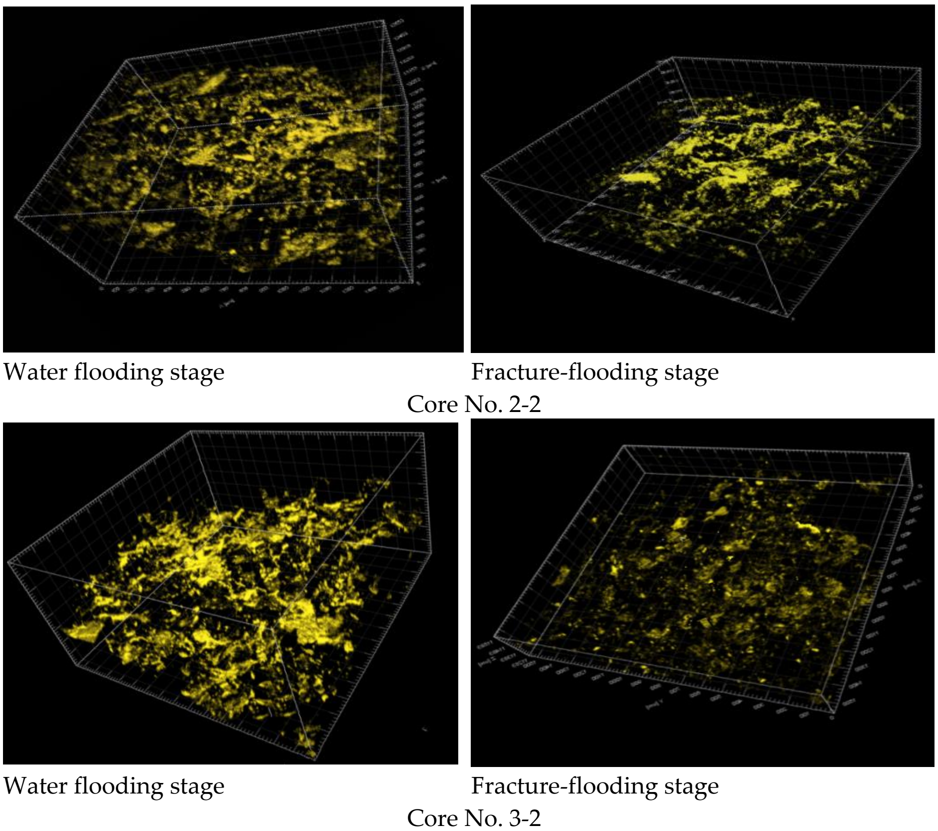

Figure 11. Three-dimensional distribution map of the remaining oil in cores at different displacement stages using confocal scanning laser.

It can be seen from the data in Table 4 that in the water flooding stage, the recovery degree is low and the remaining oil content is high. Among them, the remaining oil content of membrane- and column-like, cluster-like, intergranular-adsorption-like, and particle-adsorbent-like type remaining oil is high, accounting for 80.63% of the remaining oil saturation. In the fracture flooding stage, the production effects of the membrane- and column-like and cluster-like types of remaining oil on the pore surface are the best, and the residual oil saturation decreases from 8.89% and 15.75% to 4.95% and 12.54%, followed by the degree of intergranular-adsorption-like, throat-like, and corner-shaped types remaining oil, and the residual oil saturation decreases from 6.47%, 2.36%, and 4.48% to 5.83%, 1.45% and 3.32%.

Figure 12 shows the comparison of the remaining oil content of different types after water flooding and fracture flooding. The content of the membrane-like and column-like and cluster-like types of remaining oil on the pore surface after fracture flooding is the highest mainly because: (1) For membrane-like and column-like types of remaining oil on the pore surface, the binding property of crude oil in the hole wall of the oil-wet core during water flooding is strong. Water displaces oil from the middle pore, and the pore wall of crude oil does not flow, resulting in the formation of the membrane-like and column-like types of remaining oil on the pore surface. On the one hand, the high viscosity of fracturing fluid (surface active agent) increases the tangential friction force between the surface active agent and crude oil and overcomes the hole wall adhesion of crude oil, resulting in the use of membrane-like and column-like typed remaining oil on the surface of the hole. On the other hand, the surfactant can reduce the interfacial tension and change the wettability of the core, thus reducing the adhesion of the pore wall, resulting in the separation of column-shaped remaining oil on the pore surface. (2) For cluster-like type remaining oil, due to the heterogeneity of core oil and water flow degree difference, the referential passage is formed within the rock core after water is seen at the exit end, resulting in the formation of the cluster-like type remaining oil in the mainstream area that cannot be displaced by water flooding. Due to the high viscosity of fracturing fluid (surface active agent), the oil/water flow ratio is reduced, thus improving the displacement pressure, expanding the swept area, and displacing cluster-like type remaining oil.

Table 4. Relative percentage of remaining oil distribution.

Core No.	Displacement State	Recovery Degree (%)	S_o (%)						
			Bound Remaining Oil			Semi-Bound Remaining Oil		Free Remaining Oil	
			Membrane- and Column-like Type Remaining Oil	Particle-Adsorbent-like Type	Slit-like Type	Corner-Shaped Type	Throat-like Type	Cluster-like Type	Intergranular-Adsorption-like Type
1-2	Water flooding	35.94	10.24	7.08	2.20	3.16	1.59	15.53	5.91
	Fracture-flooding	52.84	6.13	5.88	1.65	2.02	1.03	13.25	4.32
2-2	Water flooding	36.36	8.51	6.36	1.22	4.93	2.52	17.56	6.29
	Fracture-flooding	49.84	4.17	6.08	0.91	3.82	1.44	12.53	4.95
3-2	Water flooding	33.38	7.91	5.96	2.68	5.35	2.96	14.17	5.26
	Fracture-flooding	48.56	4.54	5.52	2.09	4.12	1.89	11.84	4.25
AVG	Water flooding	35.23	8.89	6.47	2.03	4.48	2.36	15.75	5.82
	Fracture-flooding	50.41	4.95	5.83	1.55	3.32	1.45	12.54	4.51

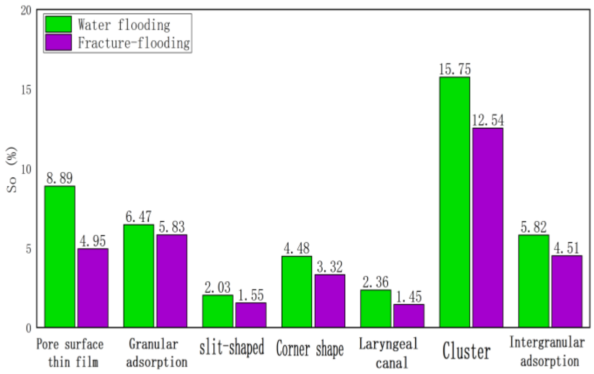

Figure 12. Comparison of remaining oil content of different types of a confocal scanning laser.

The remaining oil in intergranular-adsorption-like type, throat-like type and corner-shaped type remaining oil has a high exploitation degree, which is mainly because the remaining oil in intergranular adsorption form is mainly distributed in the position with high clay content and under the high displacement speed of fracture flooding and the partial remaining oil in the intergranular adsorption form is utilized. The remaining oil in the throat form is mainly due to the small displacement pressure difference between the two sides of the throat during water flooding, resulting in the inability of the remaining oil to flow. After fracturing fluid (surfactant) injection, the remaining oil in the throat-like type is reduced due to solubilization. The surfactant can increase displacement pressure difference, reduce interfacial tension, and effectively displace the remaining oil in throat-like type. The corner-shaped remaining oil is highly exploited due to the particularity of its position (with one side being closed). Thus, effective displacement cannot be achieved in the blind end during water flooding, while fracturing fluid (surface active agent) emulsifies the remaining oil in the inlet side of the blind end into droplets by solubilization and then displaces the residual oil. In addition, the increased viscosity of fracturing fluid increases the tangential tension of the remaining oil of the corner-shaped type so that it is more likely to be exploited.

Particle-adsorbent-like and slit-like residual oil are mainly residual oil in the bound state, which has a relatively low utilization degree and poor displacement effect.

3.2.3. CT Scanning Technology

(1) Experimental Method

Microcomputer tomography [34] (micro-CT) is used in this experiment, which scans the core after displacement, obtains the X-ray attenuation coefficient data of each substance in the scanning area, and reconstructs the data volume in three dimensions. The image processing was adjusted (adjust the threshold brightness, remove noise, and improve beam hardening), and professional software was used to realize image segmentation and pore network model establishment. The fluid and rock skeleton particles of each phase were segmented and extracted from the image and the model, and the distribution maps of oil, water, and particle phases in the core were obtained. The micro residual oil was classified based on Euler number, contact ratio, and shape factor of oil cluster. During the whole experiment, the position of the core holder in the CT scanner remained unchanged, which means in situ scanning was used.

(2) Experimental Procedures

- Core preparation: Natural cores of class III reservoir layers were selected and dried at 110 °C, and core permeability, porosity, and other basic physical parameters were measured. After vacuumizing, the core was saturated with water first and then with oil. The CT scan was performed on the core in the initial bound water state to obtain the scanning data volume.
- Water flooding: The displacement speed was 0.1 mL/min. The displacement would be stopped when no oil was produced at the producing side. CT scan was performed on the core to obtain the scanning data volume.
- Fracture-flooding: Surfactant will be reversely injected at high pressure (2 MPa) to play a displacement role (injected at the production side of water flooding). Displacement speed was 0.6 mL/min, with an injection volume of 0.3 PV; the core was scanned by CT to obtain scan data volume.

The description of micro remaining oil in core: CT scan data were processed and analyzed to perform the three-dimensional reconstruction.

(3) Morphological Characterization of Microscopic Remaining Oil Occurrence

- Occurrence types of microscopic residual oil

After the data volume obtained from the CT scan was analyzed and processed, the scanning image was generated and the three-dimensional remaining oil distribution map was reconstructed. According to factors such as the occurrence location, oil–water contact relationship, and flow morphology of microscopic remaining oil, it can be divided into five types [35,36]: cluster-like, multi-porous form, column-like, droplet-like, and membrane-like, according to the contact ratios, Euler numbers, and shape factors of oil clusters, as shown in Table 5.

Table 5. Quantitative characterization of the microscopic remaining oil.

Type	Typical Figure	Number of Occupied Pore-Throat	Shape Factor	Contact Ratio	Euler Number
clustered-like	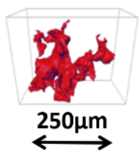	Connected Pore Number > 5	G > 2	C ≥ 0.4	EN ≤ −1
multi-porous form	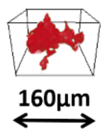	1 < Connected Pore Number ≤ 5	G > 2	C ≥ 0.4	EN > −1

Table 5. emphCont.

Type	Typical Figure	Number of Occupied Pore-Throat	Shape Factor	Contact Ratio	Euler Number
columnar-like	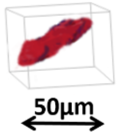	Number of Pore-Throat ≤ 1	G > 2	C $\geq$ 0.4	EN > 0
droplet-like	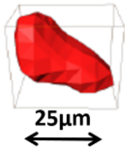	Number of Pore-Throat ≤ 1	G $\leq$ 2	C = 0	EN > 0
membranous-like	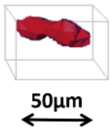	Thickness< 1/3 of pore-throat diameter	G > 2	C < 0.4	EN > 0

- Distribution of remaining oil in the two-dimensional plane by CT scanning

The core in different displacement stages (initial stage, water flooding, and fracture flooding stages) was scanned by tomography, and 600 sections were scanned in each stage. After the scanning, data should be reconstructed and a reasonable area should be selected for image plane optimization. The optimization process mainly includes: adjusting threshold brightness, removing noise, and improving beam hardening. The two-dimensional CT images of core in different displacement stages are shown in Figures 13 and 14. In the two figures, the red area is the oil phase, the blue area is the water phase, and the gray area is rock particles.

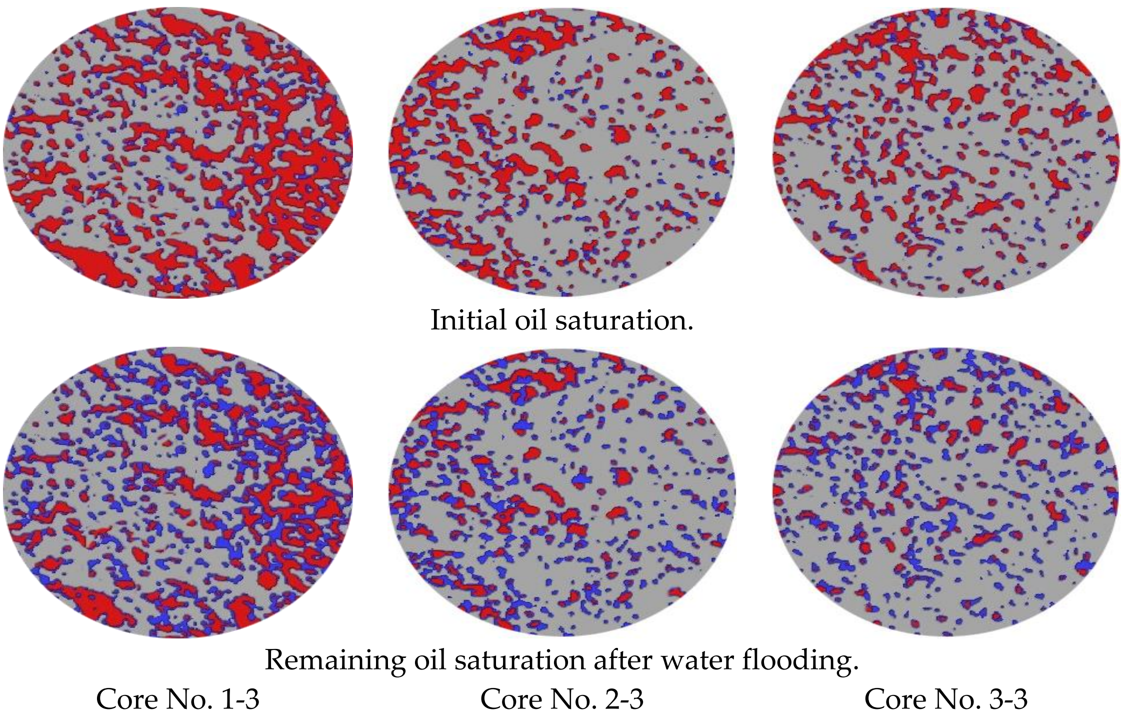

Figure 13. Two-dimensional distribution map of remaining oil during the water flooding stage constructed after CT scan.

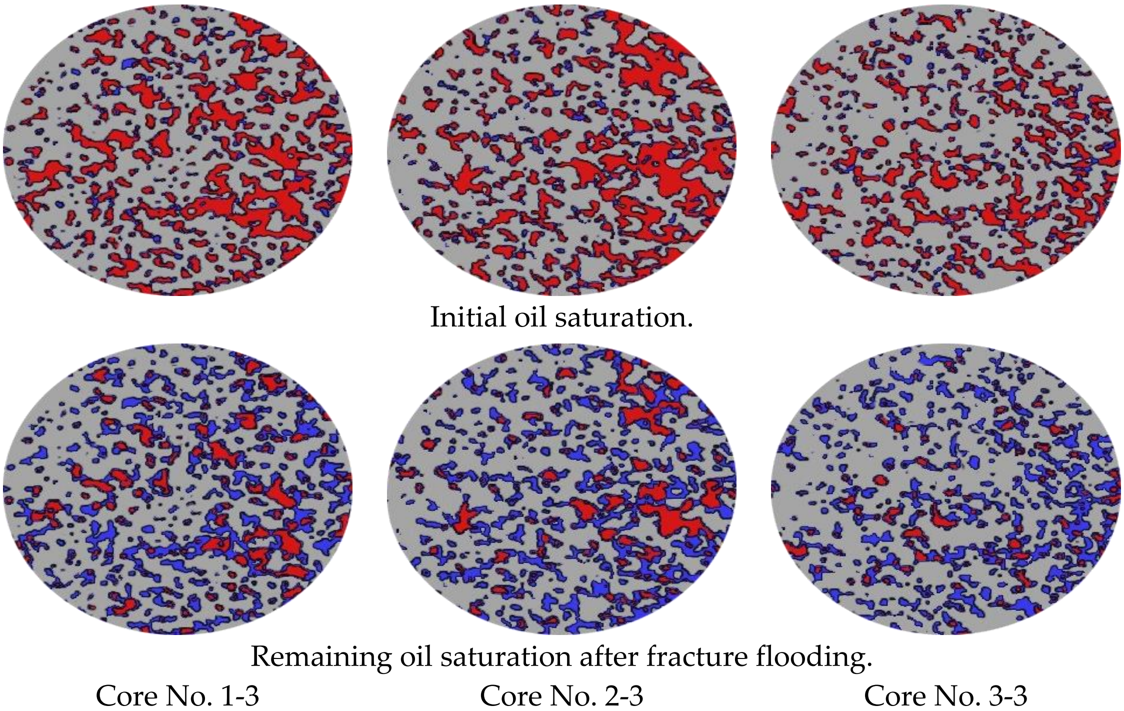

Figure 14. Two-dimensional distribution map of remaining oil during the fracture flooding stage constructed after CT scan.

In the initial state of core (bound water), the crude oil was mainly composed of continuous-phase microscopic residual oil (cluster-like and multi-porous form), with a little discontinuous-phase microscopic residual oil (column-like, droplet-like, and membrane-like). In the water flooding stage, the crude oil was displaced, washed, segmented, and dispersed by the water phase, and the crude oil gradually changed from continuous-phase to discontinuous-phase. The proportion of remaining oil with column-like, droplet-like, and membrane-like types gradually increased, but that of the remaining oil with continuous phase (cluster-like and multi-porous form) in the pores was still high due to the water-flooding fingering phenomenon. At the fracture flooding stage, due to reverse fracture flooding (where the surface active agent was injected into the production side), the affected area was extended, and the continuous-phase residual oil was displaced, and the surface active agent could reduce the interfacial tension, increase the viscosity of fracture fluid, and enhance the shearing action within the pore percolation. Thus, the membrane-like residual oil decreased significantly, some droplet-like remaining oil was produced effectively, and the residual oil saturation was further reduced.

- The construction of the three-dimensional model of remaining oil distribution after CT scanning

The cores at different displacement stages were scanned by CT. After the data volume was obtained, it was denoised and trivalued to construct a three-dimensional pore network model (Figure 15, the red area is oil phase; the blue area is water phase) to study and analyze the distribution morphology of microscopic remaining oil and carry out the quantitative characterization, as shown in Table 6, Figure 16.

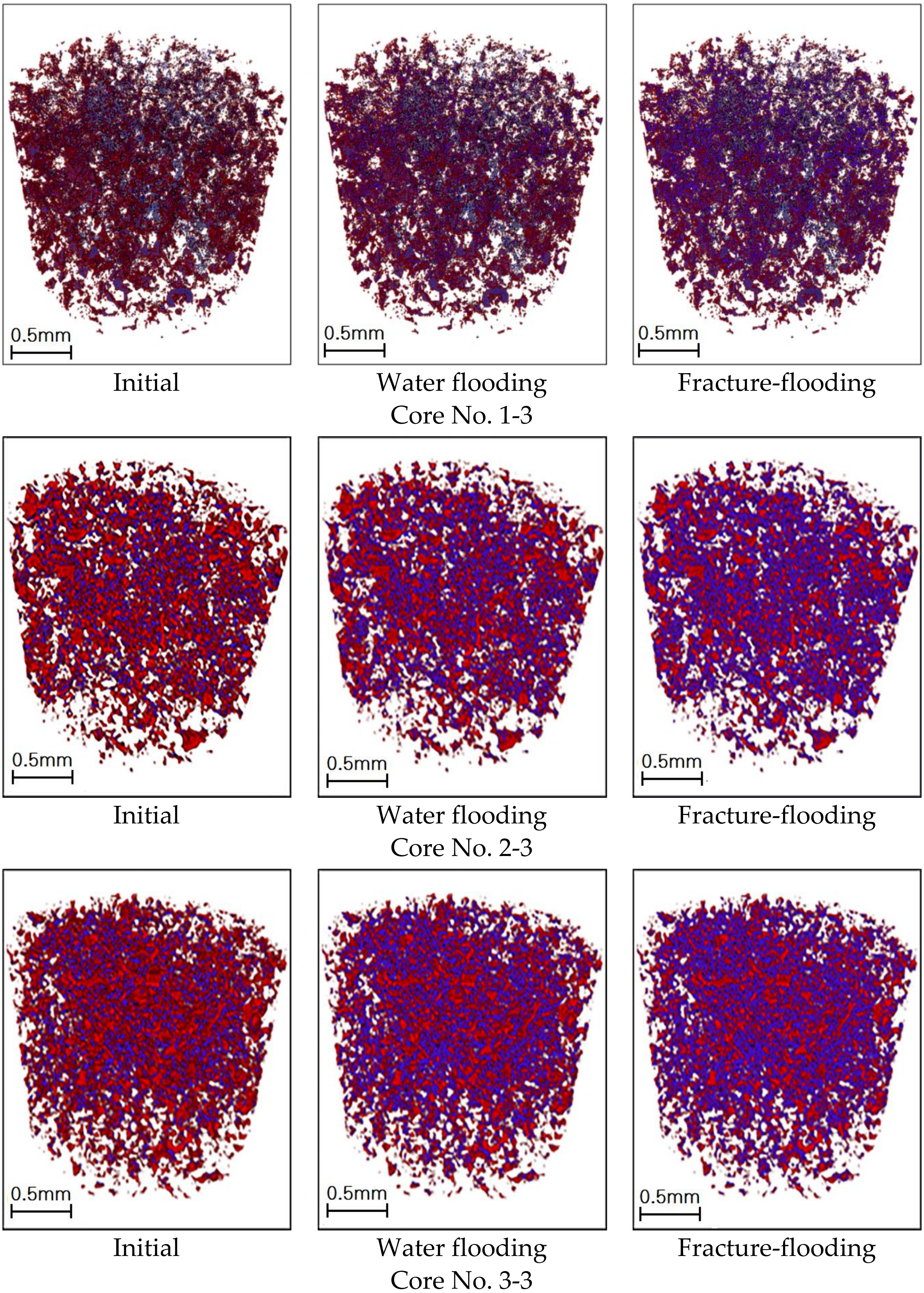

Figure 15. Three-dimensional distribution map of remaining oil constructed after CT scan.

Table 6. Data table of microscopic remaining oil distribution content after CT scan.

Well No.	Core No.	Displacement State	Oil Saturation, S_o (%)	Remaining Oil Saturation (%)				
				Cluster-like	Multi-Porous Form	Column-like	Droplet-like	Membrane-like
G111-J455	1-3	The initial	68.72	38.68	18.89	1.56	5.14	4.45
		Water flooding	43.83	12.34	8.55	5.08	7.53	10.33
		Fracture-flooding	33.46	10.12	8.28	4.53	5.67	4.86
N5-21-741	2-3	The initial	65.61	32.41	23.46	3.59	3.98	2.17
		Water flooding	42.34	14.23	9.32	3.76	5.79	9.24
		Fracture-flooding	34.47	12.46	7.16	5.92	4.74	4.19
X2-1-729	3-3	The initial	67.11	33.95	24.76	2.62	3.03	2.75
		Water flooding	40.83	14.48	9.45	4.24	5.89	6.77
		Fracture-flooding	34.58	13.15	9.16	4.87	4.34	3.06
The mean		The initial	67.15	35.01	22.37	2.59	4.05	3.12
		Water flooding	42.33	13.68	9.11	4.36	6.40	8.78
		Fracture-flooding	34.17	11.91	8.20	5.11	4.92	4.04

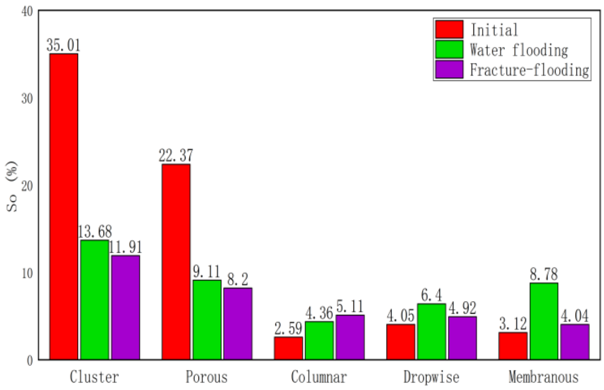

Figure 16. Comparison of remaining oil content of different types based on CT scans.

It can be seen from the constructed three-dimensional remaining oil distribution diagram that, under the condition of initial saturated oil, the bound water content is relatively low, the oil phase is the continuous phase, the saturation of cluster-like and multi-porous oil is 57.38%, and the remaining oil of the discontinuous phase (column-like, droplet-like, and membrane-like) is scattered at the corner of pore edges. In the water flooding stage, the oil phase was displaced and divided, forming a large number of droplet-like and membrane-like residual oil, but due to reservoir heterogeneity, poor oil/water viscosity, and the fingering phenomenon, the affected area of water flooding was limited. The residual oil after water flooding was mainly composed of the cluster-like and multi-porous remaining oil, with the remaining oil saturation being 22.79% and mainly occurring in the big pores and pore-throat junction. At the fracture flooding stage, due to the displacement mode (reverse fracture flooding at high speed) and the fracturing fluid (surface active agent), the viscosity of the displacement fluid and the displacement pressure difference increased, which increased the swept area, and the cluster-like and multi-porous remaining oil with continuous phase were effectively displaced. The residual oil saturation decreased to 20.11%, and the reduced interfacial tension enabled the effective displacement of the membrane-like and droplet-like remaining oil. The S_o decreased from 8.78% and 6.40% to 4.04% and 4.92% after water flooding.

4. Conclusions and Suggestion

The analysis of micro residual oil characteristics under fracture flooding shows that fracture flooding can effectively displace the residual oil in small and medium pores and the cluster-like residual oil in large pores, indicating that fracture flooding can expand the swept volume. Surfactant in fracture flooding can improve oil washing efficiency and effectively use membrane-like residual oil in pores. The results are as follows:

(1) According to NMR results, after fracture flooding, the peak value of the T_2 spectrum curve of NMR shifted to the left, the degree of middle-pore production increased from 33.13% to 49.40%, the degree of small-pore production increased from 19.09% to 40.91%, and the degree of middle- and small-pore space production increased significantly.

(2) The confocal scanning laser study showed that the membrane-like and cluster-like remaining oil on the pore surface was highly produced.

(3) CT scanning was used to quantitatively characterize the microscopic remaining oil types in each displacement stage. After fracture flooding, the displacement sweep volume increased, the cluster-like and multi-porous remaining oil with continuous phase was effectively utilized, the remaining oil saturation was reduced to 20.11%, and the reduced interfacial tension enabled the effective production of membrane-like and droplet-like remaining oil. The remaining oil saturation decreased from 8.78% and 6.40% to 4.04% and 4.92% after water flooding. The membrane-like and cluster-like remaining oil could be produced effectively.

At present, the research on the micro residual oil distribution characteristics of fracturing displacement can only simulate the process of surfactant entering matrix pores from fractures through high-speed displacement. The influence of real fractures on remaining oil should be considered in future research processes.

Author Contributions: Conceptualization and experiment, N.J. and Z.Z.; methodology G.Q.; formal analysis, J.Z.; data curation, R.Z.; writing—review and editing, N.J. and Z.Z.; project administration, N.J. and G.Q. All authors have read and agreed to the published version of the manuscript.

Funding: The project is supported by the reform and development fund of local universities supported by Heilongjiang Provincial undergraduate universities (2020YQ17). This study was supported by "Study on Water Invasion Mechanism and Seepage Law of Deep Water Gas Reservoir" (2019YDL-08) and "Research on Optimization Method of Oilfield Injection Production Strategy Based on Intelligent Optimization Algorithm" (2020YDL-25).

Conflicts of Interest: The authors declare no conflict of interest.

References

1. Du, Q.; Song, B.; Zhu, L.; Jiang, Y.; Zhao, G. Challenges and countermeasures of the waterflooding development for Lasaxing oilfields during extra-high watercut period. *Pet. Geol. Oilfield Dev. Daqing* **2019**, *38*, 189–194.
2. Lu, X.; Lu, X.; Deng, Q. Effects evaluation and mechanism analysis of enhancing oil recovery by chemical flood in type III oil reservoir in Daqing oilfield. *Pet. Geol. Oilfield Dev. Daqing* **2011**, *30*, 131–136.
3. Jia, Z.; Yang, Q.; Hou, Z.; Dong, D.; Yuan, M. EOR feasibility study on ASP flooding for classIIIoil reservoirs. *Pet. Geol. Oilfield Dev. Daqing* **2013**, *32*, 106–109.
4. Dai, X.; Wu, D.; Zhang, J.; Li, P.; Li, M. Water flooding mechanism of shallow oil horizontal hydraulic fractures and its influence on exploitation effect. *Petrochem. Ind. Technol.* **2018**, *25*, 107–109.
5. Tan, F.Q.; Xu, C.F.; Zhang, Y.L.; Luo, G.; Chen, Y.K.; Liu, W.T. Differences of microscopic seepage mechanisms of water flooding and polymer flooding and prediction models of final oil recovery for conglomerate reservoir. *Oil Gas Sci. Technol.* **2019**, *74*, 13. [CrossRef]
6. Chen, Y.; Jha, N.K.; Al-Bayati, D.; Lebedev, M.; Sarmadivaleh, M.; Iglauer, S.; Saeedi, A.; Xie, Q. Geochemical controls on wettability alteration at pore-scale during low salinity water flooding in sandstone using X-ray micro computed tomography. *Fuel* **2020**, *271*, 117675. [CrossRef]
7. Liu, Z.; Cheng, H.; Xu, C.; Chen, Y.; Chen, Y.; Li, Y. Effect of lithology on pore-scale residual oil displacement in chemical flooding using nuclear magnetic resonance experiments. In Proceedings of the SPE EOR Conference at Oil and Gas West Asia, OnePetro: 2018, Muscat, Oman, 26–28 March 2018.
8. Liu, R.; Pu, W.; Ushakova, A.; Ren, H.; Du, D.; Luo, Q.; Gou, R.; Luan, H. Micro-Displacement Mechanism of Divalent Cations Activated Polymer Flooding in A Complex Conglomerate. In Proceedings of the SPE Russian Petroleum Technology Conference, OnePetro: 2019, Moscow, Russia, 22–24 October 2019.
9. Liang, Y.; Li, Z.; Li, J.; Sun, X. Distribution of Microscopic Remaining Oil after ASP Flooding in Saertu Oilfield in Daqing. In Proceedings of the International Field Exploration and Development Conference, Xi'an, China, 18–20 September 2018; Springer: Berlin, Germany, 2018; pp. 1653–1662.

10. Xia, H.; Wang, L.; Han, P.; Cao, R.; Zhang, S.; Sun, X. Microscopic Residual Oil Distribution Characteristics and Quantitative Characterization of Producing Degree Based on Core Fluorescence Analysis Technology. *Geofluids* **2021**, *2021*, 8827721. [CrossRef]
11. Li, W.; Wei, F.; Xiong, C.; Ouyang, J.; Zhao, G.; Shao, L.; Dai, M. A novel binary compound flooding system based on DPG particles for enhancing oil recovery. *Arab. J. Geosci.* **2019**, *12*, 1–12. [CrossRef]
12. Zhou, Z.; Zhang, F.; Liu, B.; Liu, J. Microscopic Residual Oil seepage Mechanism and Pore Throat Producing Characteristics in High Water-Cut Reservoirs. *Xinjiang Geol.* **2021**, *39*, 275–279.
13. Gao, H.; Cheng, Y.; Wang, X.; Li, T.; Yang, L. Experiment of microscopic water displacement mechanism based on NMR displacement technology in nultra-lowpermeabilitys and stone. *Prog. Geophys.* **2015**, *30*, 2157–2163. (In Chinese)
14. Bai, Z.; Wu, S.; Fu, Z. The distribution of microcosmic remaining oils after polymer flooding in Daqing oil field. *Acta Pet. Sin.* **2013**, *34*, 924–931.
15. Liu, Y.; Fan, M.; Zhang, D.; Wang, F.; Liang, S.; Zhao, X. Microscopic characteristics of the remained oil after ASP flooding. *Pet. Geol. Oilfield Dev. Daqing* **2015**, *34*, 117–120.
16. Xu, Q. Distribution characteristics of the micro-remained oil after ASP flooding in Daqing Oilfield. *Pet. Geol. Oilfield Dev. Daqing* **2019**, *38*, 110–116.
17. Wang, L.H.; Xia, H.F.; Han, P.H.; Cao, R.B.; Sun, X.D.; Zhang, S.Q. Microscopic characteristics of remaining oil distribution and quantitative characterization of its producibility. *Lithol. Reserv.* **2021**, *33*, 147–154.
18. Zhang, S. Change laws of the pore structure and micro-residual oil for the polymer/surfactant composite flooding at different displacement stages. *Pet. Geol. Oilfield Dev. Daqing* **2020**, *39*, 98–104.
19. Xia, H.F.; Li, W.Z.; Liu, Y.; Zhang, H.Y.; Xu, T.H. Quantitative analysis of residual oil after weak alkali ASP flooding. *Sci. Technol. Eng.* **2019**, *19*, 127–131.
20. Liu, L.L.; Wang, L.H.; Yang, S.R.; Fan, J.W.; Wang, C.Y. Study on residual oil displacement by microporous polymer solution. *J. Eng. Thermophys.* **2018**, *39*, 348–354.
21. Jinbu, L.; Shuangfang, L.; Guohui, C.; Junfeng, S.; Yingjie, H.; Junli, M. Friability evaluation for the mud shale reservoirs based on the mineralogy and rock mechanics. *Pet. Geol. Oilfield Dev. Daqing* **2015**, *34*, 159–164.
22. Chaoyang, X.; Zhi, L.; Meie, L.; Yuekang, Z. Fracturing technology for exploiting potential of thin and poor reservoir in Daqing Oilfield. *Fault-Block Oil Gas Field* **1997**, *63*, 53–56.
23. Fangjun, B.; He, L.; Shicheng, Z.; Jin, Z.; Xiuxi, W. A numerical study of parameter influences on horizontal hydraulic fractures. *Eng. Mech.* **2011**, *28*, 228–235.
24. Jia, B.; Chen, Z.; Xian, C. Investigations of CO_2 storage capacity and flow behavior in shale formation. *J. Pet. Sci. Eng.* **2021**, *208*, 109659. [CrossRef]
25. He, J.; Wang, H. Design and effect of fracture-flooding in Class III oil reservoirs. *J. Southwest Pet. Univ. (Sci. Technol. Ed.)* **2018**, *40*, 95–104.
26. Ma, Y. Type III oil reservoirs in Daqing Placanticline oilfield. *Pet. Geol. Oilfield Dev. Daqing* **2021**, *40*, 103–109.
27. Teng, Q.; Yang, Z.; Liu, X.; Xiong, S.; Feng, C. Physical Simulation of Water Flooding in Plate Model Similar Theory Study. *Sci. Technol. Eng.* **2013**, *13*, 2478–2482.
28. Liu, G.; Pang, F.; Chen, Z. Development of scaling laws for hydraulic fracture simulation tests. *J. Univ. Pet. Nat. Sci. Ed.* **2000**, *24*, 45–48.
29. He, Y.; Mao, Z.; Xiao, L.; Ren, X. An improved method of using NMR T2 distribution to evaluate pore size distribution. *Chin. J. Geophys.* **2005**, *48*, 412–418.
30. Li, H.; Zhu, J.; Guo, H. Methods for Calculating Pore Radius Distribution in Rock from NMR T2 Spectra. *Chin. J. Magn. Reson.* **2008**, *25*, 273–279.
31. Mao, W.; Jia, H.; Du, P. Application of NMR in the study of oil/water two phase flow. *Spec. Oil Gas Reserv.* **2011**, *18*, 103–105.
32. Wang, W.; Yi, X.; Yin, D. Microscopic remaining oil distribution in ultra-low permeability reservoir by laser confocal method—By taking Fuyang reservoir of Yushulin oilfield as an example. *Pet. Geol. Eng.* **2021**, *35*, 50–55.
33. Sun, X.; Li, Y.; Dai, Q. Laser scanning confocal microscope in micropores study. *J. Chin. Electron. Microsc. Soc.* **2014**, *33*, 123–128.
34. Rosenberg, E.; Lynch, J.; Gueroult, P.; Bisiaux, M.; De Paiva, R.F. High Resolution 3d Reconstructions of Rocks and Composites. *Oil Gas Sci. Technol.* **1999**, *54*, 497–511. [CrossRef]
35. Li, J.; Jiang, H.; Wang, C.; Zhao, Y.; Gao, Y.; Pei, Y.; Wang, C.; Dong, H. Pore-scale investigation of microscopic remaining oil variation characteristics in water-wet sandstone using CT scanning. *J. Nat. Gas Sci. Eng.* **2017**, *48*, 36–45. [CrossRef]
36. Li, J.; Gao, Y.; Jiang, H.; Liu, Y.; Dong, H. Pore-Scale Imaging of the Oil Cluster Dynamic during Drainage and Imbibition Using In Situ X-Ray Microtomography. *Geofluids* **2018**, *2018*, 7679607. [CrossRef]